Journal of Fluorescence (2019) 29:15–25
https://doi.org/10.1007/s10895-018-2304-6

ORIGINAL ARTICLE

On the Discoloration of Methylene Blue by Visible Light

A. Sáenz-Trevizo[1] · P. Pizá-Ruiz[1] · D. Chávez-Flores[2] · J. Ogaz-Parada[2] · P. Amézaga-Madrid[1] · A. Vega-Ríos[1] · M. Miki-Yoshida[1]

Received: 5 July 2018 / Accepted: 14 October 2018 / Published online: 26 October 2018

Abstract

The discoloration of methylene blue in aqueous solution was studied under illumination by a fluorescent lamp, LEDs of red, green, and blue light, and a UV-A black light bulb. Overall results showed that methylene blue was discolored with and without the presence of any photoactive semiconductor. Outcomes depended on the combination substrate-light source employed. Photosensitization was assumed as the discoloration mechanism followed upon visible light irradiation. Fluorescence spectroscopy and high-performance liquid chromatography were used to investigate the possible intermediates formed in the irradiated solutions. The detailed nature of formed species was not stablished, but it was proved that the dye molecule photo-bleached and partially defragmented in several intermediates including leuco dyes, demethylated phenothiazine dyes, and probably humic substances. Since the fluorescence intermediates found were similar for most of the irradiated solutions, it was assumed that comparable reactive species were responsible for the discoloration of the molecule in solution. Results proved the misconception of discoloration experiments found in the literature when employing visible light near the absorption region of the dye.

Keywords Methylene blue · Photosensitization · Fluorescence intermediates · Type I mechanism

Introduction

The photo-assisted decomposition of organic pollutants has been adopted as a method to evaluate the photocatalytic activity of certain materials [1–14]. Authors employ dyes such as methylene blue (MB) [8–14], alizarin red [1], rhodamine B [2], orange II [5], and indigo carmine [15], among others, to monitor the photocatalytic efficiency. Nevertheless, it has been proposed that a different degradation pathway of the dyes takes place when wavelengths in the UV or visible interval are used for these experiments [1–7]. Findings suggest that conversely to photocatalytic degradation, photosensitization of the dyes occurs when visible light is employed [8, 12, 13, 15–23]. Such transformation has been associated to the characteristic region of absorption of these dyes in the visible range. As a result of absorption, a phenomenon that triggers intersystem crossing or energy transfer within the target molecule proceeds. Such process derives in the generation of reactive species, including the production of highly reactive singlet oxygen or hydroxyl radical. These species are presumably similar to the ones formed by the interaction of electrons and holes that arise from the excitation of semiconductors. The presence of these species could therefore cause the transformation of the dyes. Notwithstanding, a controversy about the true photocatalytic or non-photocatalytic nature of the reactions involved within the use of these substances has arisen [4, 6, 24]. Authors argue that only discoloration (partial degradation) instead of mineralization of the dye takes place when photocatalyst / dye systems are exposed under a light source. In consequence, it has been suggested that standard photocatalytic tests based on dyes discoloration (only optically) should be avoided [6, 7, 24]. Until now, several groups continue to analyze possible visible light activated photocatalyst and photoactive nanostructures in order to clarify such interrogatives [11, 25, 26]. On the other hand, researchers have redirected attention towards the study of other materials that can act as photosensitizers, e.g. porphyrins, metal complexes, semiconductors [16, 17, 27] and composites [19, 28]. These studies are based on the well-known oxidizing

Electronic supplementary material The online version of this article (https://doi.org/10.1007/s10895-018-2304-6) contains supplementary material, which is available to authorized users.

✉ M. Miki-Yoshida
mario.miki@cimav.edu.mx

[1] Centro de Investigación en Materiales Avanzados S.C., Miguel de Cervantes 120, Chihuahua C.P. 31136, Mexico

[2] Facultad de Ciencias Químicas, Universidad Autónoma de Chihuahua, Circuito No. 1 Campus Universitario, C.P. 31125 Chihuahua, Mexico

power of the reactive species produced upon photosensitization [8, 12, 13, 17, 19–23, 27].

Conventional broadband light sources such as Xenon or Mercury lamps are commonly used to evaluate the photocatalytic property of materials. However, the different wavelengths provided can interfere in their interaction with the dye-material and present long-term power instability. Therefore, it is believed that within the utilization of monochromatic or nearly monochromatic light sources [7, 11, 16, 22, 29–34], the reduction of time required for the transformation of the target pollutants is achieved [29, 33] and a more reliable assessment of the interaction of dye-irradiation source-material can be attained.

This work summarizes the effect of different illumination sources in the UV and visible wavelengths onto aqueous MB solutions in contact with bare borosilicate glass (BGS) substrates. A sample of Ti oxide coated ZnO nanorods grown onto BGS glass was employed for comparative purposes. After all irradiation experiments, the amount of MB solutions discoloration was calculated, and the irradiated solutions (degraded products) were studied by fluorescence spectroscopy (FS) and high-performance liquid chromatography (HPLC). The later with the aim to monitor the progressive changes of the MB molecule as studied by Tsuchiya et al. only with UV irradiation [35], here the wavelength interval was extended to the visible region. The analysis of the products made possible to determine if degradation or photo-bleaching of the dye occurred after being exposed to the various light sources.

Materials and Methods

Microstructure and Optical Properties

Clean pieces of BGS were used as non-reactive surfaces to study the discoloration of MB. In addition, a sample comprised of TiO_x coated ZnO nanorods deposited onto BGS (sample T) was used in further experiments. The nanostructured materials were grown via aerosol assisted CVD (AACVD) method. Synthesis conditions, reactants, and system configuration used for the preparation of sample T were reported elsewhere [36, 37]. Surface morphology of sample T was studied by field emission scanning electron microscopy (SEM) in a JEOL JSM-7401F operated at a voltage of 2 kV. The microstructure of the sample T was analyzed by high-resolution scanning transmission electron microscopy (HR-STEM) in a JEOL JEM-2200FS microscope equipped with a spherical aberration probe corrector. The equipment was operated at an accelerating voltage of 200 kV. ZnO nanorods of sample T were scratched directly on TEM grids. The total transmittance and reflectance spectra of the BGS substrate and sample T were measured in the 300 to 1000 nm interval, using a UV-Vis-NIR CARY 5000 spectrophotometer with a DRA2500 integrating sphere accessory.

Characterization of the Light Sources

Different light sources were employed for the discoloration experiments: a commercial 15 W fluorescent lamp (F15T8D), and three commercial LEDs. A black light bulb (F15T8BLB, named BLB) of emission in the UV-A region, was employed for further comparative purposes. The qualitative emissions provided by the fluorescent lamp and each LED were estimated with a Thorlabs CCS200 compact spectrophotometer coupled to a multimode optic fiber (active in the range from 200 nm to 1000 nm). The irradiance of the individual LEDs was determined using a Thorlabs PM100D spectrophotometer equipped with a Thorlabs S120VC power sensor of 50 mW and 9.5 mm of diameter that works in the 200 to 1100 nm interval. The number of photons provided by each illumination device was computed from irradiance measurements.

Dye Discoloration Tests

The discoloration of aqueous solutions of MB at an initial concentration of 10^{-5} mol.dm^{-3} was studied as a function of irradiation time using different light sources. The pH of the prepared MB solutions had a value of 4. The experiments were carried out employing 5 cm^3 and 10 cm^3 of the probe solution; for both a teflon ring reactor was employed to enclose the probe solution. The ring had 21 mm of internal diameter and 19 mm (for 5 cm^3) or 31 mm (for 10 cm^3) of height. The ring reactors were bounded at the bottom with a tightly attached clean piece of BGS or sample T, and covered at the top with a fused quartz cover to protect the MB solution. The ring reactor containing the MB solution was placed onto a supporting platform inside of an irradiation chamber. A small eccentric mass attached to a DC motor rotating at 2582 ± 40 rpm was placed under the platform to promote the continuous agitation of the probe solution over the essayed surfaces.

Initial discoloration experiments were carried out using the BGS substrates exposed to the different light sources. Additional tests performed with the BGS substrate and sample T were accomplished using solely the UV-A light source. The exposition time was set to 960 min for all trials. Since the values of irradiance of the light sources differed at a great extent when set at the same distance from the detector, each LED was located at a different distance from the BGS in order to balance the amount of incident light with that provided by the fluorescent lamp (30 W.m^{-2}). The temperature of the chamber was in the range of 294–310 K.

Absorbance spectra of all MB solutions were measured in a 200 to 800 nm interval in a UV-Vis-NIR CARY 5000 spectrophotometer using a 1 cm quartz cuvette. The MB absorbance peak located at 664 nm was correlated to dye concentration and was monitored as an indicator of the discoloration efficiency.

The computation of the photonic efficiencies was achieved following Eq. 1.1, employing the discoloration tests data and the values of irradiance of the different quasi monochromatic sources at λ. Effective photonic efficiency $\varepsilon_{ph}(\lambda)$ describes the number of reactant molecules transformed or product molecules formed divided by the number of *incident* photons, at a given wavelength [38]:

$$\varepsilon_{ph}(\lambda) = \frac{\#moleculesconverted}{\#incidentphotons(\lambda)} \quad (1.1)$$

Analyses of Irradiated MB Solutions Using Fluorescence Spectroscopy and High-Performance Liquid Chromatography

The effect of each light source on the MB solutions was monitored using FS and HPLC. The fluorescence emissions of irradiated solutions were acquired with a Horiba Fluorolog-3 modular spectrofluorometer that utilizes a 450 W Xenon CW lamp as the excitation source. Samples were contained in a 1 cm path length quartz cell at room temperature (298 K). The interval of excitation wavelengths was from 300 nm to 700 nm using increments of 25 nm. The interval of emission wavelengths was from 300 nm to 800 nm with steps of 5 nm. A 5 nm slit was used for excitation wavelengths, while a 1 nm slit was used for emitted wavelengths. The irradiance of the spectrofluorometer was obtained at different wavelengths (from 335 nm to 687 nm) using the Thorlabs PM100D spectrophotometer and related sensor (as described in "Characterization of the light sources" section), in order to correlate the intensity of the fluorescence emissions of the dye with the number of photons provided by the excitation source. Further analyses of the dye discoloration products were achieved via reverse phase chromatography in a HPLC-DAD Thermo Scientific Ultimate 3000 series. The products were separated using an Acclaim 120 C18 column (150 mm X 4.6 mm) that was kept at 20 °C. The detection system was a diode array detector (DAD) that works in the range from 200 nm to 800 nm. The signals acquired by the detector were recorded in a Chromeleon Chromatography Data System software. The isocratic mobile phase consisted of two solutions namely eluent A and eluent B. Eluent A was made of trifluoroacetic acid in water (0.01% *v*/v) while eluent B was methanol. The sample injection volume was 80 μL and the flow rate was 1 $mL.min^{-1}$.

Results and Discussion

Microstructure and Optical Properties of the Samples

The morphology and crystalline structure of sample T used as reference are shown in Fig. 1. Top surface SEM micrograph in

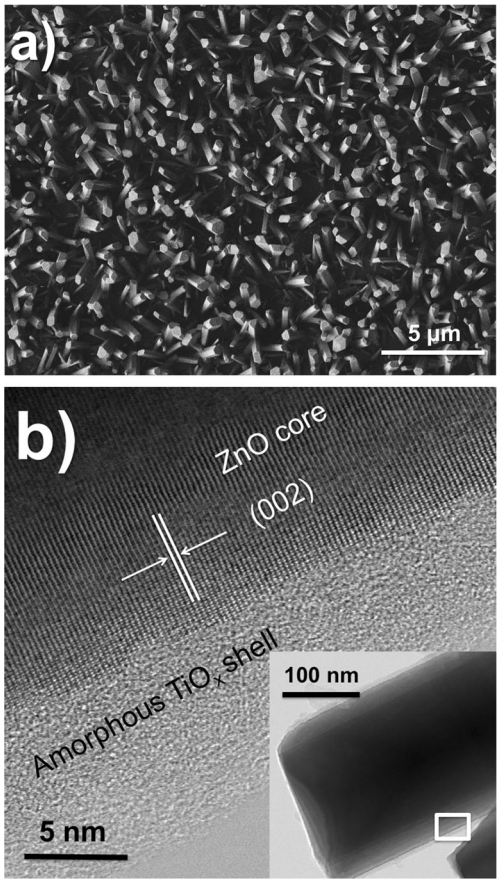

Fig. 1 **a** Secondary electron SEM micrograph of the surface of sample T. **b** HR-STEM micrographs of sample T. The inset shows the analyzed zone in b)

Fig. 1a exhibits elongated structures having a hexagonal cross-section morphology. The depicted shape matched with the formation of one-dimensional nanorods. Lattice fringes observed in the HR-STEM micrograph of scratched nanorods of sample T (see Fig. 1b) confirmed the crystalline characteristic of the nanostructures. This information was in agreement with the formation of monocrystalline ZnO wurtzite [39]. Furthermore, the evident development of a thin layer (having a thickness of 15 ± 4 nm) of amorphous Ti oxide grown onto the ZnO nanorods was noted. Inset in Fig. 1a shows the existence of the TiO_x coating. All attributes were in accordance with the information reported earlier in [36, 37] for ZnO-TiO_x core-shell materials. Sample T was selected as a reference because the integrity of the ZnO core was preserved after several extended tests performed in an aqueous medium [37]. Besides, the photocatalytic activity obtained with sample T was similar to that obtained using bare ZnO nanorods.

The absorptance spectra of the bare BGS glass and sample T are shown in Fig. 2. Both spectra were obtained from total transmittance and reflectance measurements. Figure 2 evidenced that the region of absorption of the BGS glass differed to a great extent from that of the nanostructured sample T. Bare BGS exhibits a negligible absorption in the visible

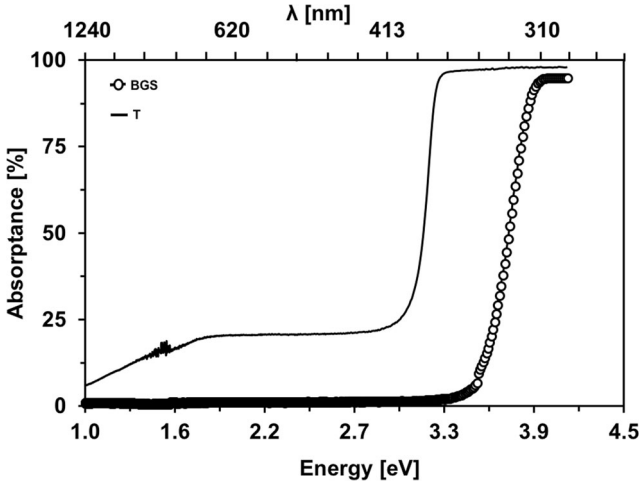

Fig. 2 Optical absorptance as a function of photon energy of the BGS substrate and sample T

interval but important in the UV region above 3.5 eV. On the other hand, sample T exhibited a sharp absorption edge at around 3.2 eV (congruous with the existence of the synthesized metal oxides) and optical absorption of about 20% to 5% extending from the visible to the infrared region. Outcomes confirmed that the BGS substrate does not interact with wavelengths in the visible region, as those provided by the light sources in Online Resource 1.

Characteristics of the Light Sources

Details of total irradiance and qualitative spectra of fluorescent (FL) and black light (BLB) lamps were reported previously in reference [37]. The spectral emissions of the each LED were located at around 633 ± 15 nm, 527 ± 23 nm and 467 ± 16 nm; and their irradiance at 1 cm from the detector were 275 $W.m^{-2}$, 45 $W.m^{-2}$, and 115 $W.m^{-2}$ for the red, green, and blue LED, respectively. The total irradiance of the FL lamp at the same distance from the detector was 31 $W.m^{-2}$, which is quite different from the irradiances of the LEDs. Thus, due to these different irradiances each LED was positioned at different distance to guarantee the same irradiance onto the MB solution. The qualitative spectral irradiance of FL lamp and each LEDs appear in Online Resource 1.

Dye Discoloration Tests

Discoloration experiments were performed with 10 cm^3 of MB solutions in contact with pristine BGS substrates using the different light sources. Outcomes appear summarized in Table 1. For comparative purposes, the experimental run also comprised outcomes obtained using a UV-A light source to irradiate the MB solution.

As noted in Table 1, an important amount of the dye was transformed upon irradiation with the fluorescent

Table 1 Total incident photons into the illuminated area of the reactor ($3.46\ 10^{-4}\ m^2$) during 960 min.; percent of MB discolored (D) and effective photonic efficiencies (ε_{pht}) obtained using a bare BGS substrate irradiated with different light sources

Light source	Incident photons (μmol)	D (%)	ε_{pht} (10^{-4}%)
Fluorescent lamp	–	44 ± 2	–
Red LED(633 nm)	3066	57 ± 4	19 ± 2
Green LED (527 nm)	2553	16 ± 1	6 ± 5
Blue LED (467 nm)	2262	5 ± 1	2 ± 1
UV-A	–	6 ± 1	–

lamp and the red LED. Interestingly, the red LED yielded 13% of more discoloration than that obtained with the fluorescent lamp. The discoloration observed using the UV-A light and the green and blue LEDs was less favorable than that obtained with the red LED and the fluorescent device. Photonic efficiencies showed that when normalizing the amount of irradiance, the red LED exhibited more discolored molecules for incident photon, following the order: ε_{pht} red LED> ε_{pht} green LED> ε_{pht} blue LED. Foregoing outcomes could be related to the amount of absorbed light by the MB solution. According to the absorbance spectra of the probe solution (shown in Fig. 3), the blue and green LEDs are barely absorbed. The absorbance of the blue, green, and red LED emission, were of 0.020 ± 0.001, 0.030 ± 0.004, and 0.40 ± 0.02, respectively. Such measured values of absorbance indicated that even when the photons in the blue and green regions were more energetic than those in the red region, their limited absorption has a restricted influence on the discoloration of the dye. In addition, it is known that the absorbance peaks of MB, shown in Fig. 3, at about 293 nm and

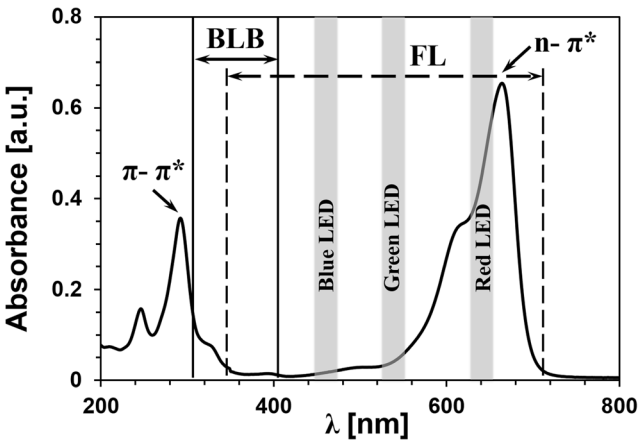

Fig. 3 Absorbance spectrum of the MB probe solution. It is shown the absorbance peaks associated with π – π* and n – π* transitions of the MB. Additionally, the different wavelength range emitted by the fluorescent lamp (FL), the LEDs (blue, green, and red) and the UV-A lamp (BLB) are included

664 nm are associated with π – π* and n – π* transitions, respectively [40]. In consequence, the utilization of photons close or at these wavelengths would excite the molecules of the dye.

Conveniently, photosensitization from either Type I or Type II mechanisms [12, 16–18, 20, 21] along with the absorption of light at certain spectral regions (as shown in Fig. 3), could serve to explain the effective discoloration of MB with visible light. According to literature, Type I or Type II mechanisms take place when the molecule of the dye is excited (i.e. when n – π* transitions occur). Type I mechanism involves an electron or H_2 atom abstraction by the excited state of the sensitizer (in this case MB). Type II mechanism involves the energy transfer from the excited sensitizer to the ground state of O_2 [16]. In consequence, the generation of reactive oxygen species and free radicals, both occurring under irradiation with visible light (as the one provided by the red LED and the FL lamp, see Fig. 3 and Online Resource 1), could support the effective discoloration of MB. Outcomes matched with the results of reference [22], which summarized the discoloration of several photosensitizers (including MB) under irradiation with red light. The limited discoloration observed using the blue and green LEDs, which are scarcely absorbed by MB, could be also elucidated.

On the other hand, it has been proved that singlet oxygen produced from MB can be satisfactorily used to degrade organic substances. For instance, Stojicic et al. [12], Komine and Tsujimoto, [20] and Huang et al. [21] applied singlet oxygen from MB as a bactericidal agent. Pena-Luenga et al. [16] showed that upon irradiation of this dye, the decomposition of various organic pollutants in solution was achieved. However, it is worth mentioning that the generation of singlet oxygen is sometimes overestimated. This is because the formation of free radicals (commonly associated with Type I process) can occur together with the formation of singlet oxygen. Therefore, it was difficult to attribute the degradation of the MB molecules (and transformation of pollutants) to either of the photosensitization mechanisms. Moreover, the progress of both mechanisms relies upon the lifetime (quantum yield) and stability of the excited states of the dye, aside from the absorption of light in the spectral region of excitation [8, 16–18]. The investigation of these parameters is needed in order to verify the effectiveness over time of the employed wavelengths.

Since the evident transformation of MB solution took place without the presence of a photocatalyst, further tests with duration of 960 min were carried. In this case, 5 cm^3 of the MB solution in contact with pristine BGS and sample T were illuminated with a BLB. The results of this test appear summarized in Table 2.

Results in Table 2 showed that the combination of the black light bulb and photoactive semiconductors in sample T (that absorb photons in the UV-A region, see Fig. 2) had a favorable effect in the discoloration of the dye. In fact, almost a complete discoloration (95%) of the probe solution was observed. For solution in contact with the BGS substrate, the low percent of discoloration was consistent with the tests in Table 1 and those presented in a previous work [37]. In this case, findings revealed that the UV-A light source did not produce the photosensitization and discoloration of the dye. Consequently, results of nanostructured sample T suggested that photocatalytic transformation of the dye occurred. The process was originated due to an effective excitation of electron and holes and its interaction with the surrounding aqueous media. No significant differences on the discoloration of MB solutions were observed when the black light bulb was employed to irradiate 10 or 5 cm^3 of solution. The analysis of the tested solutions was performed to set differences among the products formed, as described in the following sections.

Table 2 Amount of MB solution discolored after 960 min of exposure to the UV-A source

Samples	D (%)
T	95 ± 3
BGS	7 ± 2

Analysis of the MB Solution

Fluorescence Emissions of MB Solution

The fluorescence emissions of the probe solution of MB were investigated in the interval of 300 nm to 800 nm. The measured emissions appear in Fig. 4. In Fig. 4a, an intense characteristic emission peak at about 685 nm - 690 nm was observed using excitation of 300 nm (FWHM 30 nm). The identified peak matched with that reported for the fluorescence of MB [8, 35, 41]. Furthermore, three other constant emissions were detected accompanying the MB peak. The peak at 300 nm (partially shown) correspond to elastic scattering from the excitation wavelength; the second peak at 335 nm was associated to the Raman signal of water [41, 42]; the third peak at 600 nm was attributed to second order scattering of the excitation wavelength [42]. Online Resource 2 revealed that the emission associated with MB (685 nm - 690 nm), as well as those resulting from elastic scattering and Raman signal of water, were evident using all excitation wavelengths (from 325 nm to 700 nm). Figure 4b shows that the intensity of the characteristic emission peak of MB was modified when the excitation wavelengths increased. Three zones of maximal emission were noted: 300 nm, 600 nm - 620 nm and 685 nm - 690 nm. Alternatively, a low intensity emission region between 350 nm to 525 nm was observed. Fig. 4b also shows that the emissions at 685 nm and 690 nm were almost identical. A narrower step might be suitable to improve the resolution of the maxima. Furthermore, the emission of the characteristic peak of MB was not dependent on the irradiance of the

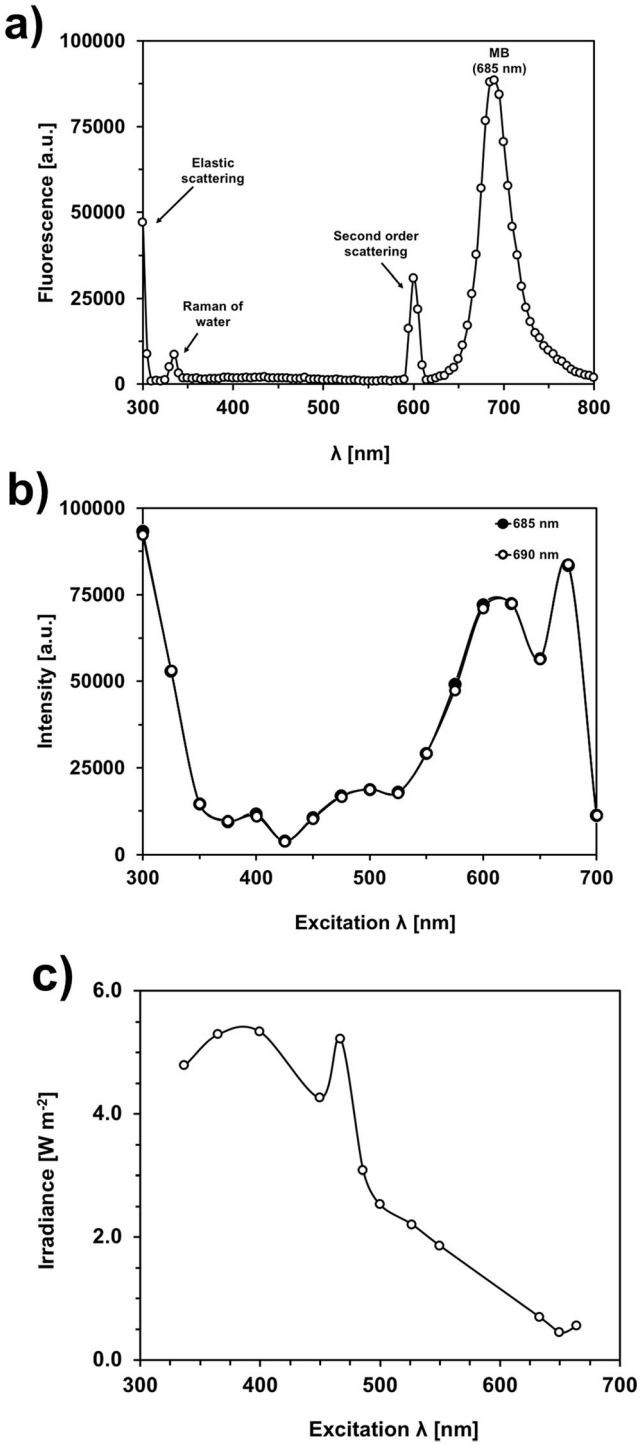

Fig. 4 Fluorescence emissions of MB solution. **a** Emission spectrum of MB probe solution obtained with 300 nm of excitation; **b** intensity of the fluorescence emissions located at 685 nm and 690 nm as a function of excitation wavelengths and **c**) spectral irradiance emitted by the spectrofluorometer source

selected wavelengths. Figure 4c shows the irradiance of several excitation wavelengths provided by the spectrofluorometer source. As noted, the irradiance of the excitation wavelengths decreased when using lower energy photons (longer wavelengths). Outcomes in Fig. 4b, c suggested that in spite of the decreasing excitation intensity, wavelengths above 575 nm could excite the molecule of the dye, i.e. photosensitization of MB could take place (as explained in "Dye discoloration tests" section). Such observations were in contrast with the very low emission observed at 400 nm, which exhibited the highest excitation intensity. Since clear differences in the collected emissions using excitation wavelengths of 300 nm and 400 nm, both wavelengths were used for all of the following fluorescence studies.

Aforementioned observations revealed that not all wavelengths had the same capacity to excite the fluorescent state of the MB molecule in water, in accordance with the absorbance spectrum of MB shown in Fig. 3.

Fluorescence Emissions of Irradiated MB Solutions

The fluorescent spectra of irradiated MB solutions (Table 1) in contact with the borosilicate glass substrate, and exposed to a fluorescent lamp, red LED (rLED), and UV-A bulb were obtained in order to determine the emissions of the products formed after irradiation. Emissions recorded at excitation wavelengths of 300 nm and 400 nm are presented in Fig. 5a, b, respectively.

For excitation at 300 nm, the emissions recorded from the irradiated solution using the FL, rLED, and BLB showed a decrease in the emission of the MB characteristic peak located at 685 nm (see Fig. 5) in comparison with the non-irradiated MB solution, consistent with discoloration results of Table 1. According to Fig. 5a, new emissions of fluorescence were noted in all solutions. For the solution after exposure to the fluorescent lamp, a shoulder located close to 450 nm (FWHM 85 nm) was observed. A barely intense shoulder located at around 425 nm (FWHM 90 nm) appeared in the solution irradiated with the red LED. In addition, a low intense emission was noticed in the solution irradiated with the black light bulb centered at about 420 nm (FWHM 90 nm) and closely matches the peak of MB used as reference. Additionally, the Raman peak of water at 335 nm and the second order scattering at 600 nm appear invariants in all cases.

Emissions obtained using 400 nm as a source of excitation revealed further information about the transformation of the dye. As shown in Fig. 5b, the solutions exposed under the FL and rLED showed intense signals centered at 565 nm (FWHM 85 nm and FWHM 95 nm, respectively). A slight shift of the characteristic peak to 680 nm (FWHM 90 nm) was also noticed in both cases. For the solution irradiated with the black light bulb it was found an analogous but less intense shoulder at 565 nm (FWHM 60 nm) and, no shift of the MB peak. Observed peaks at nearby 680 nm and 565 nm are congruent with those reported by Tsuchiya et al. [35] as fluorescence characteristics peaks during the decomposition of MB, using an excitation of 365 nm. In addition, the Raman signal of

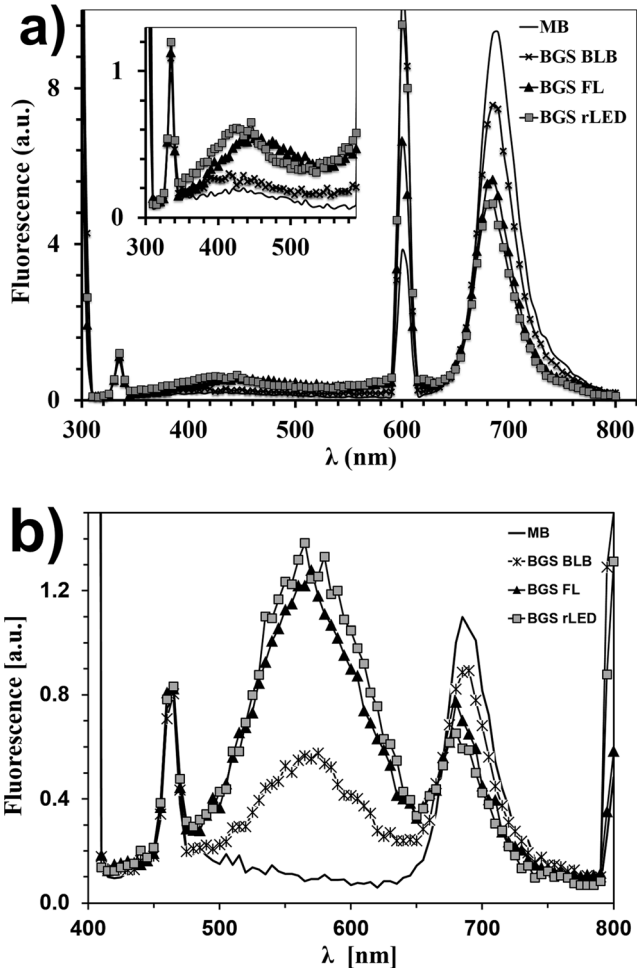

Fig. 5 Fluorescence emissions of irradiated MB solutions in contact to the BGS excited at: **a**) 300 nm and **b**) 400 nm. Inset in a) shows details at the low wavelength region

water along with the second order scattering signals appeared invariant at 465 nm and 800 nm, respectively. Results showed that in spite of the different amount of MB discoloration with the various light sources, analogous residues can be expected.

Based on the results described in "Dye discoloration tests" section (Table 1), the partial discoloration of MB solution in contact with pristine borosilicate glass substrate was possible using the FL, rLED and BLB light sources. In addition, Fig. 5 evidences the formation of similar fluorescence residues. For experiments carried out using a red LED and the fluorescent lamp, it is suggested that photosensitization of the MB solution occurred since the wavelength range supplied by both sources was coincident with the high absorption interval of the MB (600 nm - 690 nm). In the case of BLB irradiation, the proximity of provided wavelength interval and the absorption region of the MB at higher energies (240 nm - 300 nm) can explain the observed minor discoloration of the MB solution. On the other hand, the slightly shifted positions from 685 nm to 675–680 nm represents changes in the molecular structure occurring in several steps at different parts of the molecule as reported by Tsuchiya et al. [35] and detailed by Yu and Chuang [14]. The formation of demethylated phenothiazine dyes (of the MB family) has been recognized after performing discoloration experiments using other characterization methods [10, 14, 43].

Additional emissions occurring at about 450 nm and 565 nm indicated further information about the transformation of the dye. For those samples exhibiting fluorescence close to 450 nm, it is possible that the colorless forms of these dyes (leuco) were present in solution. The fluorescence of leuco MB molecules has been reported at 452 nm for leuco MB (LMB) and 462 nm for leuco Thionine (Th), both observed with excitation of 320 nm [41]. Nevertheless, the broad and intense shoulder centered at these wavelengths also resembles the emissions reported for humic substances dissolved in water. Humic species are mainly composed of aromatic or aliphatic carbon chains combined with nitrogen, sulfur, and oxygen atoms (all in the MB molecule) [44–46]. Emissions at 565 nm (570 nm also) have been associated with changes in the aromatic rings of the molecule, as seen in reference [35] using 365 nm of excitation. It is important to note that the emissions at 452 nm, 462 nm, and 565 nm (570 nm) were obtained using different excitation wavelengths that those presented herein. However, in order to prove that these emissions were independent of the excitation wavelength (as it occurred with the peak at 685 nm - 690 nm of MB), selected solutions were examined. Excitation wavelengths of 325 nm and 375 nm were chosen for the current study. This was carried out with the assumption that its proximity to the reported excitation wavelengths (320 nm for leuco dyes [41] and 365 nm for modification of the molecular ring structure [35]), will not result in considerable discrepancies. Online Resource 3 obtained from the different collected solutions confirmed the invariant position of the emitted shoulders of fluorescence. Therefore, outcomes indicated that the observed emissions can be used as reference. Also, the existence of broad shoulders implied that different species coexist in the irradiated MB solutions, since the width of the fluorescence peaks has been associated with heterogeneity [35].

Further information about the transformation of the dye was obtained from MB solutions (Table 2) in contact with the BGS substrate and sample T, both exposed to the black light bulb. Figure 6a shows the fluorescence spectra for an excitation of 300 nm, it is shown that the solution in contact with the pristine BGS did not display a shift of the maximum emission at 685 nm (FWHM 35 nm). Only a slight decrease of the intensity of this peak in comparison with that of the non-irradiated MB solution was seen. A broad shoulder centered at 415 nm (FWHM 120 nm) was noted, similar to the one emitted by the non-irradiated MB solution. For solution in contact with sample T, a complete disappearance of MB characteristic peak was observed. Only a shoulder centered at 405 nm (FWHM 75 nm) emerged. For excitation with 400 nm the

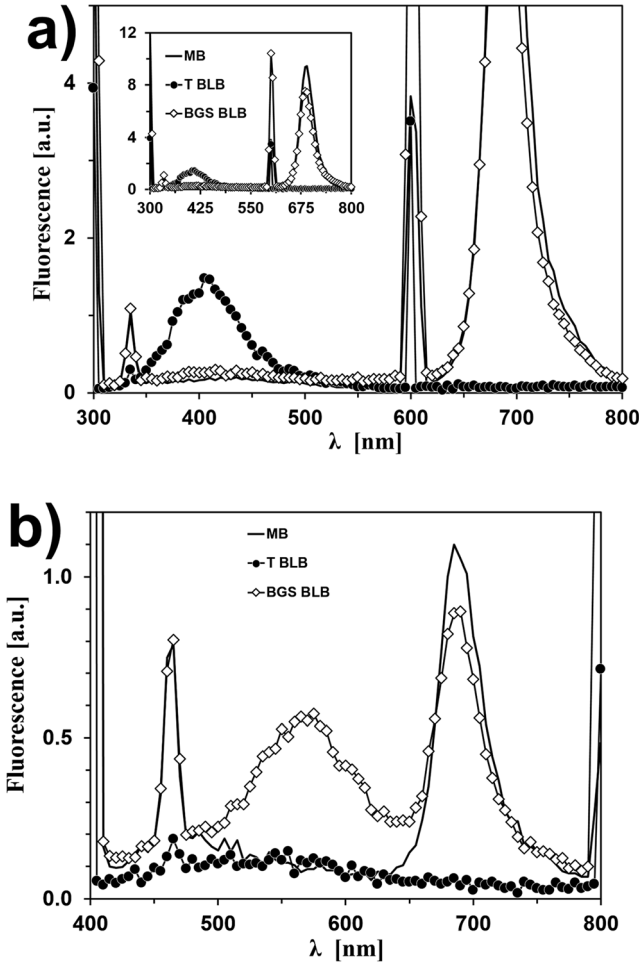

Fig. 6 Fluorescence emissions of MB solutions in contact with the pristine BGS and sample T recorded with excitation wavelengths of: **a**) 300 nm and **b**) 400 nm. Inset in a) shows details of characteristic MB peak

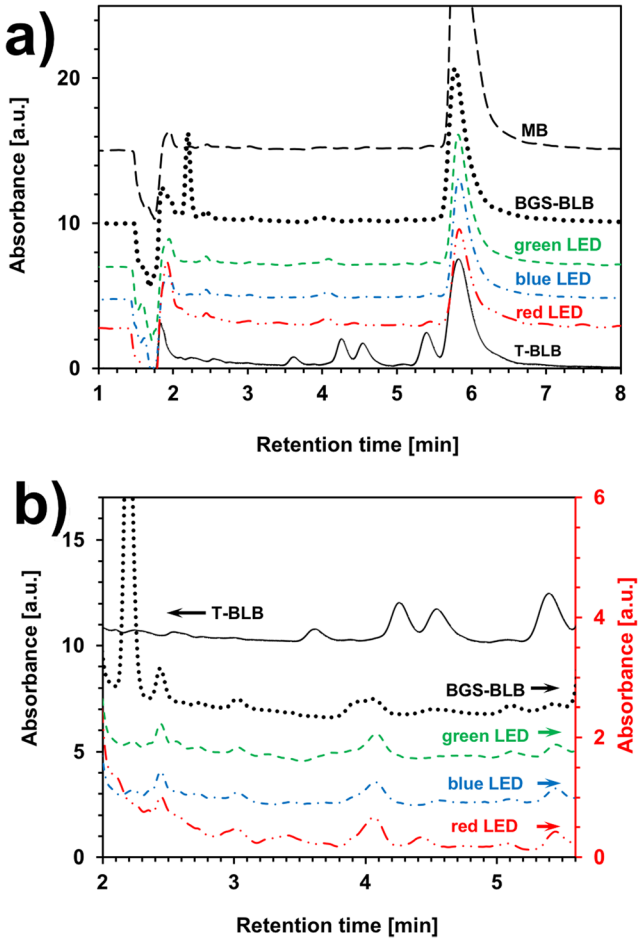

Fig. 7 HPLC-DAD chromatograms recorded at 245 or 290 nm. a) From a probe solution of MB, and solutions in contact with: borosilicate glass irradiated with black light bulb (BGS-BLB), green LED, blue LED, and red LED; and sample T irradiated with the BLB (T-BLB). b) Details in the retention time interval of 2.0–5.6 min

emissions from MB solution in contact with BGS (Fig. 6b) showed a slight decrease of the characteristic MB peak intensity, also a broad peak centered at 565 nm (FWHM 70 nm). For MB solution in contact with sample T, as in the 300 nm case a complete disappearance of MB characteristic peak, and the occurrence of one broader shoulder centered close to 550 nm (FWHM 150 nm) were noted. Concurrently, results presented in Table 2 and Fig. 6b are consistent with those reported in reference [35], it can be concluded that the MB solution in contact with sample T when irradiated with UV-A light degraded photocatalytically.

Analysis of Non-irradiated and Irradiated MB Solution Via HPLC

The chromatographic separation of MB and selected irradiated solutions was monitored over the range of 200 nm to 800 nm. Since intense signals were obtained at 245 and 290 nm, outcomes in Fig. 7 were presented using these wavelength. As seen in Fig. 7, the reference solution of MB displayed a characteristic peak at a retention time of 5.7 min. In all other solutions, the reference peak of MB remained visible, accompanied by the existence of secondary peaks at shorter retention times.

Results obtained from solution in contact with sample T exposed to a black light bulb, displayed the most intense signals at shorter retention times. These multiple peaks observed in the range from 2.5 min to 5.5 min can be related to the peaks reported by Yogi et al. [10] in the degradation of the MB molecule irradiated 120 min in contact with a TiO_2 film. Retention times in the interval of 4.0 to 5.0 min suggest species with absorbance bands of about 620 nm to 630 nm, matching with the presence of demethylated species of MB. The MB solutions in contact with borosilicate glass irradiated with BLB, green LED, blue LED, and red LED gave almost the same elution profiles for retention times larger than 2.5 min, but different to that of sample T irradiated with BLB. Peaks at about 2.5 min indicated the existence of species with absorbance bands at or below 200 nm. The peak at

2.2 min of MB solution in contact with BGS irradiated with the red LED was singular and non-identified, it is inexistent in all the other elution profiles. Signals around retention times of 1.8 min were associated with the column dead-time. It is worth mentioning that several methods have been reported for the detection of MB and its intermediates, and in all cases, different retention times have been presented. These differences were associated to the lack of a standard method (solvent, volume mixture and flow rate) for the analysis of MB by liquid chromatography or chromatography coupled with mass spectroscopy [47–49].

Online Resources 4 and 5 show the 3D chromatograms of solutions presented in Tables 1 and 2, measured in the interval of 200 nm to 800 nm. Both images revealed that the signal of MB solution could be traced with almost all wavelengths in the visible region, as in the case of fluorescence spectroscopy. However, noticeable different signals were measured at about 200 nm in all cases. This information indicates that significant changes of the molecule of MB were out of the detection limit of the DAD detector. Similar findings have been observed in the absorbance spectra of MB (obtained by UV-Vis spectroscopy), reported by other authors [26, 33, 43] and as seen in solutions presented herein (Online Resource 4). Such information proved the existence of molecules with absorbance spectra below the detection limits. Therefore, only qualitative data was obtained from HPLC.

Previous experiments [37] revealed that the $^{\bullet}OH$ radicals resulting from the interaction of holes with water are the main reactive species responsible for the transformation of MB. Likewise, it is known that the same radicals (along with $^{\bullet-}O_2$) are expected from Type I photosensitization mechanisms [13, 17, 18, 20, 21]. Because of the observed similarities, it can be assumed that for the case presented herein, reactive $^{\bullet}OH$ played a major role in the MB degradation when it was photosensitized. Despite previous evidence, Type I and Type II mechanisms [8, 13, 21, 22] can participate in the degradation process simultaneously and at different ratios [8, 13, 21, 22]. For that reason, further tests considering proper scavengers are needed in order to confirm such information.

Overall outcomes proved that a false indication about the photocatalytic degradation of MB could be determined using wavelengths in the visible range. Consequently, the replacement of the target substances used in the assessment of the photocatalytic activity has to be considered when employing irradiation sources that emit wavelengths in the region of absorption of the elected dye. Alternatively, other analytical techniques than optical absorption must be employed to evaluate the degradation of the dye. Preceding remarks are in agreement with the statements of Serpone et al. [4], Ohtani [6] and Herrmann [24]. These authors advised that the discoloration of dyes can not be always attributed to a photocatalytic degradation or mineralization process. Other experimental tests extending the irradiation time are needed in order to confirm if the photosensitization mechanism has limited effectiveness or if this mechanism can lead to the complete degradation of the dyes. The tests could be necessary since it has been stated that with the incorporation of visible light irradiation devices and visible light absorbing materials (commonly dyes), the original molecule responsible for the absorption of light (chromophore) will disappear [16]. In consequence, only the partial degradation of the intermediates could be achieved. Results also suggested that fluorescence spectroscopy and liquid chromatography can be useful to easily monitor the chemical transformation of a target molecule.

Conclusion

The photosensitization of MB resulting on its own partial degradation was effectively evidenced after irradiation with different light sources. Such transformation was more manifest when using the wavelengths provided by the red LED, which comprises photons within the most intense dye's absorption region. Fluorescence spectroscopy showed that the intermediates formed after irradiation exhibited fluorescence emissions in the visible interval. Results suggest that the dye was not only photo bleached, but also transformed into intermediates, including leuco dyes, demethylated phenothiazine dyes, and probably humic substances. Moreover, it was found that the various irradiated solutions in contact with the bare BGS and a nanostructured sample (TiO_2 coated ZnO) exhibited fluorescence emissions in the same interval of wavelengths. Thus, it was considered that such fluorescent molecules were formed by the reaction of comparable reactive species present due to the photosensitization of MB and after the photo activation of the semiconductors. On the other hand, since Type I photosensitization mechanism led to the formation of free radicals similar to the ones formed upon excitation of semiconductors, it is suggested that this mechanism had a major role in the self-degradation of the dye. Outcomes also showed that fluorescence spectroscopy and high performance liquid chromatography can be used as initial approximations to monitor the transformation of the MB. The detailed examination of the solutions is needed in order to classify the intermediates and the final species formed.

Acknowledgements The authors thank W. Antúnez-Flores, O. Solis-Canto and C. Ornelas-Gutierrez for the technical assistance. We also acknowledge to SEP-CONACYT project N° 242612 for the financial support.

Compliance with Ethical Standards

Conflict of Interest The authors declare that there is no conflict of interest.

References

1. Liu G, Wu T, Zhao J, Hidaka H, Serpone N (1999) Photoassisted degradation of dye pollutants. 8. Irreversible degradation of alizarin red under visible light radiation in air-equilibrated aqueous TiO_2 dispersions. Environ Sci Technol 33:2081–2087
2. Zhao J, Wu T, Wu K, Oikawa K, Hidaka H, Serpone N (1998) Photoassisted degradation of dye pollutants. 3. Degradation of the cationic dye rhodamine B in aqueous anionic surfactant/TiO_2 dispersions under visible light irradiation: evidence for the need of substrate adsorption on TiO_2 particles. Environ Sci Technol 32:2394–2400
3. Zhao J, Chen C, Ma W (2005) Photocatalytic degradation of organic pollutants under visible light irradiation. Top Catal 35:269–278
4. Serpone N, Emeline AV, Horikoshi S, Kuznetsov VN, Ryabchuk VK (2012) On the genesis of heterogeneous photocatalysis: a brief historical perspective in the period 1910 to the mid-1980s. Photochem Photobiol Sci 11:1121–1150
5. Chen PK, Lee GJ, Anandan S, Wu JJ (2012) Synthesis of ZnO and au tethered ZnO pyramid-like microflower for photocatalytic degradation of orange II. Mat Sci Eng B 177:190–196
6. Ohtani B (2008) Preparing articles on Photocatalysis-beyond the illusions, misconceptions, and speculation. Chem Lett 37:217–229
7. Yan X, Ohno T, Nishijim K, Abe R, Ohtani B (2006) Is methylene blue an appropriate substrate for a photocatalytic activity test? A study with visible-light responsive titania. Chem Phys Lett 429: 606–610
8. Tuite WM, Kelly JM (1993) Photochemical interactions of methylene blue and analogues with DNA and other biological substrates. Photochem Photobiol B Biol 21:103–124
9. Houas A, Laccheb H, Ksibi M, Elaloui E, Guillard C, Herrmann JM (2001) Photocatalytic degradation pathway of methylene blue in water. Appl Catal B Environ 31:145–157
10. Yogi C, Kojima K, Wada N, Tokumoto H, Takai T, Mizoguchi T, Tamiaki H (2008) Photocatalytic degradation of methylene blue by TiO_2 film and au particles-TiO_2 composite film. Thin Solid Films 516:5881–5884
11. Liu X, Yang Y, Shia X, Li K (2015) Fast photocatalytic degradation of methylene blue dye using a low-power diode laser. J Hazard Mater 283:267–275
12. Stojicic S, Amorim H, Shen Y, Haapasalo M (2013) Ex vivo killing of enterococcus faecalis and mixed plaque bacteria in planktonic and biofilm culture by modified photoactivated disinfection. Int Endod J 46:649–659
13. Sabbahi S, Alouini Z, Jemli M, Boudabbous A (2008) The role of reactive oxygen species in Staphylococcus aureus photoinactivation by methylene blue. Water Sci Technol 58:1047–1054
14. Yu Z, Chuang SSC (2007) Probing methylene blue photocatalytic degradation by adsorbed ethanol with in situ IR. J Phys Chem C 111:13813–13820
15. Vautier M, Guillard C, Herrmann JM (2001) Photocatalytic degradation of dyes in water: case study of indigo and of indigo carmine. J Catal 201:46–59
16. Pena-Luengas SL, Marin GH, Aviles K, Cruz-Acuña R, Roque G, Rodíguez-Nieto F, Sanches F, Tarditi A, Rivera L, Mansilla E (2014) Enhanced Singlet Oxygen Production by Photodynamic Therapy and a Novel Method for Its Intracellular Measurement. Cancer Biother Radiopharm 29:435–443
17. DeRosa MC, Crutchley RJ (2002) Photosensitized singlet oxygen and its applications. Coord Chem Rev 233(234):351–371
18. Ormond B, Freeman HS (2013) Dye sensitizers for photodynamic therapy. Materials 6:817–840
19. Li Y, Dong H, Li Y, Shi D (2015) Graphene-based nanovehicles for photodynamic medical therapy. Int J Nanomedicine 10:2451–2459
20. Komine C, Tsujimoto Y (2013) A small amount of singlet oxygen generated via excited methylene blue by photodynamic therapy induces the sterilization of *Enterococcus faecalis*. JOE 39:411–414
21. Huang L, Xuan Y, Koide Y, Zhiyentayev T, Tanaka M, Hamblin MR (2012) Type I and type II mechanisms of antimicrobial photodynamic therapy: an in vitro study on gram-negative and gram-positive bacteria. Lasers Surg Med 44:490–499
22. Konopka K, Goslinski T (2007) Photodynamic therapy in dentistry. J Dent Res 86:694–707
23. Pelaez M, Nolan NT, Pillai SC, Seery MK, Falaras P, Kontos AG, Dunlop PSM, Hamilton JWJ, Byrne JA, O'shea K, Entezari MH, Dionysiou DD (2012) A review on the visible light active titanium dioxide photocatalysts for environmental applications. Appl Catal B Environ 125:331–349
24. Herrmann JM (2010) Fundamentals and misconceptions in photocatalysis. J Photochem Photobiol A Chem 216:85–93
25. Pincella F, Isozaki K, Miki K (2014) A visible light-driven plasmonic photocatalyst. Light Sci Appl 3:e133–e138
26. Sohrabnezhad S (2011) Study of catalytic reduction and photodegradation of methylene blue by heterogeneous catalyst. Spectrochim Acta A 81:228–235
27. Takaheshi C, Tsujimoto Y, Yamamoto Y (2012) The effect of irradiation wavelengths and the crystal structures of titanium dioxide on the formation of singlet oxygen for bacterial killing. J Clin Biochem Nutr 51:128–131
28. Wojtoniszak M, Rogińska D, Machaliński B, Drozdzik M, Mijowska E (2013) Graphene oxide functionalized with methylene blue and its performance in singlet oxygen generation. Mater Res Bull 48:2636–2639
29. Gondal MA, Hameed A, Yamani ZH (2005) Laser induced photocatalytic splitting of water over WO_3 catalyst. Energy Sources 27: 1151–1165
30. Gomes-Silva C, Juárez R, Marino T, Molinari R, García H (2011) Influence of excitation wavelength (UV or visible light) on the photocatalytic activity of Titania containing gold nanoparticles for the generation of hydrogen or oxygen from water. J Am Chem Soc 133:595–602
31. Kwiatkowski M, Bezverkhyy I, Skompska M (2015) ZnO nanorods covered with a TiO_2 layer: simple sol–gel preparation, and optical, photocatalytic and photoelectrochemical properties. J Mater Chem A 3:12748–12760
32. Amrollahi R, Hamdy MS, Mul G (2014) Understanding promotion of photocatalytic activity of TiO_2 by au nanoparticles. J Catal 319: 194–199
33. Tayade RJ, Sivakuma Natarajan T, Bajaj HC (2009) Photocatalytic degradation of methylene blue dye using ultraviolet light emitting diodes. Ind Eng Chem Res 48:10262–10267
34. Koci K, Zatloukalová K, Obalova L, Krejikova S, Lacny Z, Apek L, Hospodkova A, Solcova O (2011) Wavelength effect on photocatalytic reduction of CO_2 by Ag/TiO_2 catalyst. Chin J Catal 32: 812–815
35. Tsuchiya N, Kuwabara K, Hidaka A, Oda K, Katayama K (2012) Reaction kinetics of dye decomposition processes monitored inside a photocatalytic microreactor. Phys Chem Chem Phys 14(14):4734–4741
36. Sáenz-Trevizo A, Amézaga-Madrid P, Pizá-Ruiz P, Antúnez-Flores W, Ornelas-Gutiérrez C, Miki-Yoshida M (2015) Single and multi-layered core-shell structures based on ZnO nanorods obtained by aerosol assisted chemical vapor deposition. Mater Charact 105:64–70
37. Sáenz-Trevizo A, Amézaga-Madrid P, Pizá-Ruiz P, Antúnez-Flores W, Ornelas-Gutiérrez C, Miki-Yoshida M (2016) Efficient and durable ZnO core-shell structures for photocatalytic applications in aqueous media. Mater Sci Semicond Process 45:57–68

38. Emeline A, Salinaro A, Serpone N (2000) Spectral dependence and wavelength selectivity in heterogeneous Photocatalysis I. experimental evidence from the Photocatalyzed transformation of phenols. J Phys Chem B 104:11202–11210
39. Joint Committee on Powder Diffraction Standards, Powder Diffraction File, International Center for Diffraction Data, Swarthmore, PA, 2011, card 01-075-1533
40. Heger D, Jirkovsky J, Klan P (2005) Aggregation of methylene blue in frozen aqueous solutions studied by absorption spectroscopy. J Phys Chem A 109:6702–6709
41. Lee SK, Mills A (2003) Luminescence of Leuco-Thiazine Dyes. J Fluoresc 13:375–377
42. Stobieka M, Hepel M (2011) Multimodal coupling of optical transitions and plasmonic oscillations in rhodamine B modified gold nanoparticles. Phys Chem Chem Phys 13:1131–1139
43. Zhang T, Oyama T, Aoshima A, Hidaka H, Zhao J, Serpone N (2001) Photooxidative N-demethylation of methylene blue in aqueous TiO_2 dispersions under UV irradiation. J Photochem Photobiol A Chem 140:163–172
44. Chen J, LeBoeuf EJ, Dai S, Gu B (2003) Fluorescence spectroscopic studies of natural organic matter fractions. Chemosphere 50:639–647
45. Sierra MMD, Giovanela M, Parlanti E, Soriano-Sierra EJ (2005) Fluorescence fingerprint of fulvic and humic acids from varied origins as viewed by single-scan and excitation/emission matrix techniques. Chemosphere 58:715–733
46. Pan Y-L (2015) Detection and characterization of biological and otherorganic carbón aerosol particles in atmosphere using fluorescence. J Quant Spectrosc Radiat Transf 150:12–35
47. Bakre PV, Volvoikar PS, Vernekar AA, Tilve SG (2016) Influence of acid chain length on the properties of TiO_2 prepared by sol-gel method and LC-MS studies of methylene blue photodegradation. J Colloid Interface Sci 474:58–67
48. Rauf MA, Meetani MA, Khaleel A, Ahmed A (2010) Photocatalytic degradation of methylene blue using a mixed catalyst and product analysis by LC/MS. Chem Eng J 157:373–378
49. Kim S-J, Ha D-J, Koo T-S (2014) Simultaneous quantification of methylene blue and its major metabolite, azure B, in plasma by LC-MS/MS and its application for a pharmacokinetic study. Biomed Chromatogr 28:518–524